Article

Not peer-reviewed version

Gut Microbiota Composition in Maintenance Hemodialysis Patients: Associations with Sex, Age, and Body Composition

Katarzyna Bąk , Michał Kowalski , Kamila Marszalek , Patrycja Olszewska , Andrzej Ossowski , Bartłomiej Grygorcewicz , Aleksandra Cader-Ptak , Leszek Domański , Violetta Dziedziejko , Ewa Kwiatkowska *

Posted Date: 3 April 2026

doi: 10.20944/preprints202604.0227.v1

Keywords: gut microbiota; hemodialysis; chronic kidney disease; body composition; gut-kidney axis

 doi:10.20944/preprints202604.0227.v1

Article

Gut Microbiota Composition in Maintenance Hemodialysis Patients: Associations with Sex, Age, and Body Composition

Katarzyna Bąk [1], Michał Kowalski [2], Kamila Marszalek [2], Patrycja Olszewska [2], Andrzej Ossowski [2], Bartłomiej Grygorcewicz [2], Aleksandra Cader-Ptak [1], Leszek Domański [1], Violetta Dziedziejko [3] and Ewa Kwiatkowska [1,*]

[1] Clinical Department of Nephrology, Transplantology and Internal Medicine, Pomeranian Medical University, 70-001 Szczecin, Poland
[2] Department of Genomics and Forensic Genetics, Pomeranian Medical University, 70-001 Szczecin, Poland
[3] Department of Biochemistry and Medical Chemistry, Pomeranian Medical University, 70-001 Szczecin, Poland
* Correspondence: ewa.kwiatkowska@pum.edu.pl

Abstract

Background/Objectives: Patients receiving maintenance hemodialysis (HD) commonly exhibit malnutrition, chronic low-grade inflammation, and metabolic disturbances. Gut dysbiosis may contribute to these abnormalities through the gut-kidney axis. This study aimed to characterize gut microbiota composition in HD patients and examine its associations with demographic, clinical, and body composition parameters. **Methods:** This cross-sectional study included 96 patients with end-stage kidney disease on maintenance HD. Clinical, laboratory, inflammatory, nutritional, and bioimpedance-derived body composition data were collected, including Malnutrition-Inflammation Score (MIS). Stool samples were analyzed for gut microbiota composition. Associations with host-related variables were assessed using alpha- and beta-diversity analyses, subgroup comparisons, and Mantel testing. **Results:** Gut microbiota showed marked inter-individual heterogeneity at the genus level, with dominant taxa including Blautia, Faecalibacterium, Streptococcus, Gemmiger, Ruminococcus, Escherichia-Shigella, and Enterococcus. Chao1 richness was higher in men than in women. Shannon entropy and Chao1 richness were positively associated with age and visceral adipose tissue (VAT), while Faith's phylogenetic diversity increased with age. In contrast, the Gini index was negatively associated with age and VAT, indicating a more even microbial structure in older individuals and those with higher visceral adiposity. Beta-diversity differed between men and women and across categories within the female subgroup. Mantel testing showed a modest but significant correlation between microbiota and metadata distances**. Conclusions:** Gut microbiota in maintenance HD patients is highly heterogeneous and associated mainly with sex, age, visceral adiposity, and overall host phenotype. These findings suggest that microbiota variation in HD reflects multidimensional host-related factors rather than a single clinical feature**.**

Keywords: gut microbiota; hemodialysis; chronic kidney disease; body composition; gut-kidney axis

1. Introduction

Chronic kidney disease (CKD) represents a growing global health burden and a major contributor to cardiovascular morbidity and mortality. In Poland alone, approximately 4.5 million individuals are affected. Patients who progress to stage 5 CKD require kidney replacement therapy, most commonly maintenance intermittent hemodialysis (HD). In Poland, nearly 20,000 patients undergo chronic HD treatment. Despite advances in dialysis technology and supportive care,

 doi:10.20944/preprints202604.0227.v1

mortality among hemodialysis patients remains alarmingly high, reaching up to 30% within two years of follow-up [1].

Malnutrition and chronic inflammation are highly prevalent in this population and are strongly associated with adverse outcomes. Protein–energy wasting (PEW) affects up to 75–90% of patients receiving dialysis, while a persistent low-grade inflammatory state is observed in nearly all individuals undergoing HD. The interrelationship between malnutrition, inflammation, and cardiovascular disease is conceptualized as the malnutrition–inflammation–atherosclerosis (MIA) syndrome—a complex and often fatal condition in end-stage renal disease (ESRD), in which these interdependent factors coexist and mutually amplify one another, leading to accelerated vascular disease and excess mortality. MIA is frequently described as a vicious cycle, where each component exacerbates the others.

Malnutrition (M), typically defined as protein–energy wasting, is characterized by hypoalbuminemia, reduced body mass, and loss of skeletal muscle mass. Inflammation (I) is reflected by elevated circulating markers such as C-reactive protein (CRP), interleukin-6 (IL-6), and tumor necrosis factor-α (TNF-α). Atherosclerosis (A) represents accelerated vascular injury and remains the leading cause of death in dialysis patients [2].

The pathogenesis of MIA syndrome is multifactorial. Chronic inflammation in HD patients is driven by retention of pro-inflammatory uremic toxins—including indoxyl sulfate and p-cresyl sulfate—which promote sustained immune activation and endothelial dysfunction [3–5]. Additional contributors include vascular access-related infections and complications [6], as well as dialysis-related inflammatory stimuli triggered by blood–membrane interactions, dialysate contaminants, and nutrient losses during treatment [10–12]. Comorbidities such as diabetes, obesity, pre-existing atherosclerosis, chronic infections, and psychosocial factors including depression further potentiate systemic inflammation and worsen metabolic reserve [11,12].

Dietary restrictions imposed on dialysis patients—particularly limitations of fluid, sodium, potassium, and phosphorus intake—often lead to insufficient caloric and protein consumption. Depression, common in this population, may additionally suppress appetite. Moreover, each hemodialysis session is associated with amino acid and iron losses [13], and the procedure itself promotes a catabolic state, partly mediated by inflammatory signaling [14]. Chronic inflammation and malnutrition together accelerate atherosclerosis, creating a self-reinforcing feedback loop that worsens clinical prognosis.

In recent years, growing attention has been directed toward the gut–kidney axis as a central mechanism linking CKD to systemic inflammation and cardiovascular disease. CKD and ESRD are consistently associated with gut dysbiosis characterized by reduced microbial diversity, depletion of beneficial short-chain fatty acid (SCFA)-producing bacteria, and enrichment of taxa capable of generating precursors of uremic toxins. Colonic microbial metabolism substantially contributes to circulating levels of indoxyl sulfate, p-cresyl sulfate, and trimethylamine-N-oxide (TMAO), metabolites that accumulate as renal function declines and are associated with endothelial dysfunction, oxidative stress, and increased cardiovascular risk [15–17].

Mechanistically, CKD-associated dysbiosis is accompanied by increased intestinal permeability (“leaky gut”), facilitating translocation of endotoxins and other microbial products into the circulation, thereby amplifying systemic immune activation. Concurrently, reduced SCFA production may impair intestinal barrier integrity and anti-inflammatory immune pathways, including regulatory T-cell responses, further reinforcing chronic inflammation and metabolic disturbances relevant to protein–energy wasting and cardiovascular injury [15].

Emerging multi-omics and translational evidence supports the concept of a “toxic microbiome” in CKD, in which progressive enrichment of uremic toxin-producing species and depletion of protective taxa accompany disease advancement. Experimental studies demonstrate that fecal microbiota transplantation from CKD patients increases circulating uremic toxin levels and exacerbates kidney fibrosis in animal models, suggesting that gut microbial alterations may actively contribute to CKD progression rather than merely reflect it [18].

 doi:10.20944/preprints202604.0227.v1

Collectively, these findings provide a biologically plausible link between gut dysbiosis, systemic inflammation, metabolic imbalance, and accelerated atherosclerosis—key components of MIA syndrome. However, despite increasing recognition of the gut–kidney axis in CKD, the relationship between gut microbiota composition and the clinical manifestations of MIA in maintenance hemodialysis patients remains insufficiently characterized.

In the present study, we evaluated the composition of the gut microbiota in patients undergoing maintenance hemodialysis and investigated its association with nutritional status, inflammatory burden, and the occurrence of major adverse cardiovascular events, including mortality.

2. Materials and Methods

Study Design and Ethical Approval

This study was approved by the Bioethics Committee of the Pomeranian Medical University in Szczecin (approval number KB-006/17/2025). All participants provided written informed consent before inclusion.

A total of 96 patients with stage 5 chronic kidney disease undergoing maintenance intermittent hemodialysis (HD) at the Independent Public Clinical Hospital No. 2 of the Pomeranian Medical University in Szczecin were enrolled. The study consisted of four main components:

Blood sampling for the assessment of inflammatory and nutritional markers

Stool collection for gut microbiota analysis

Body composition analysis

Nutritional assessment using the Malnutrition-Inflammation Score (MIS)

Eight-month prospective follow-up for all-cause and cardiovascular mortality and major adverse cardiovascular events (MACE)

Baseline characteristics of the study population are presented in Table 1. The flow chart of participant recruitment is shown in Figure 1.

Table 1. Group characteristics.

Variable	Overall participants
Overall participants	n = 96
Women	n = 34 (35.4%)
Men	n = 62 (64.6%)
Age [years]	Median: 66; IQR = 51.0-73.3
Dialysis vintage [months]	Median: 25.5; IQR = 14.0-46.3
Patients' nutrition by BMI [%]	Underweight: n = 0 (0.0%); Normal weight: n = 43 (44.8%); Overweight: n = 31 (32.3%); Obese: n = 22 (22.9%)
FMI [kg/m²]	Median: 8.2; IQR = 4.0-11.5
FFMI [kg/m²]	Median: 19.3; IQR = 17.2-21.4
SMM [kg]	Median: 25.1; IQR = 19.9-29.8
VAT [L]	Median: 2.3; IQR = 0.9-4.4
PhA	Median: 4.5; IQR = 3.9-5.5
TBW [%]	Median: 52.7; IQR = 46.0-61.1
ERI [IU/kg/g/dL/week]	Median: 9.27; IQR = 4.14-18.68
IL-6 [pg/mL]	Median: 6.92; IQR = 3.90-12.29
hsCRP [mg/L]	Median: 4.5; IQR = 2.3-17.3
IL-1β [pg/mL]	Median: 0.04; IQR = 0.00-0.16
TNF-α [pg/mL]	Median: 2.77; IQR = 2.24-3.65
Albumin [g/L]	Median: 40; IQR = 37.0-41.0
Transferrin [g/L]	Median: 1.76; IQR = 1.55-2.02
Kt/V	Mean: 1.29 ± 0.25
Total MIS score	Median: 5; IQR = 4.0-9.0

 doi:10.20944/preprints202604.0227.v1

Abbreviations: IQR—interquartile range, BMI—body mass index, ERI—erythropoietin resistance index, MIS—malnutrition inflammation scale, Kt/V — dialysis adequacy index, MACE – major cardiovascular event

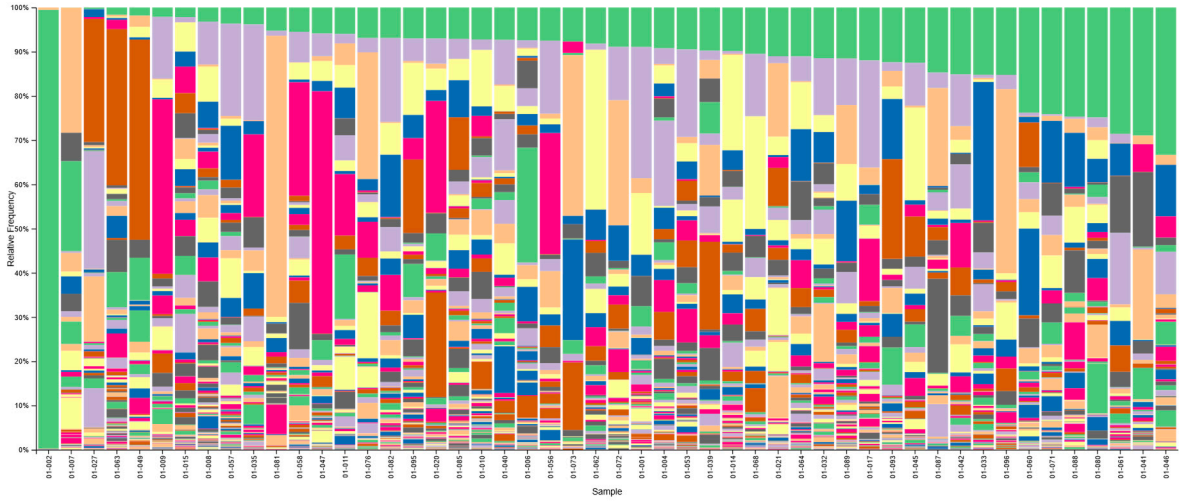

Figure 1. Stacked bar plot showing the relative abundance of taxa at the genus taxonomic level across individual samples. Each bar represents a single sample, and the total height of each bar corresponds to 100% of the microbial community composition. Different colors indicate different taxa, and their proportions reflect relative abundance. The plot illustrates variation in taxonomic composition among samples.

 doi:10.20944/preprints202604.0227.v1

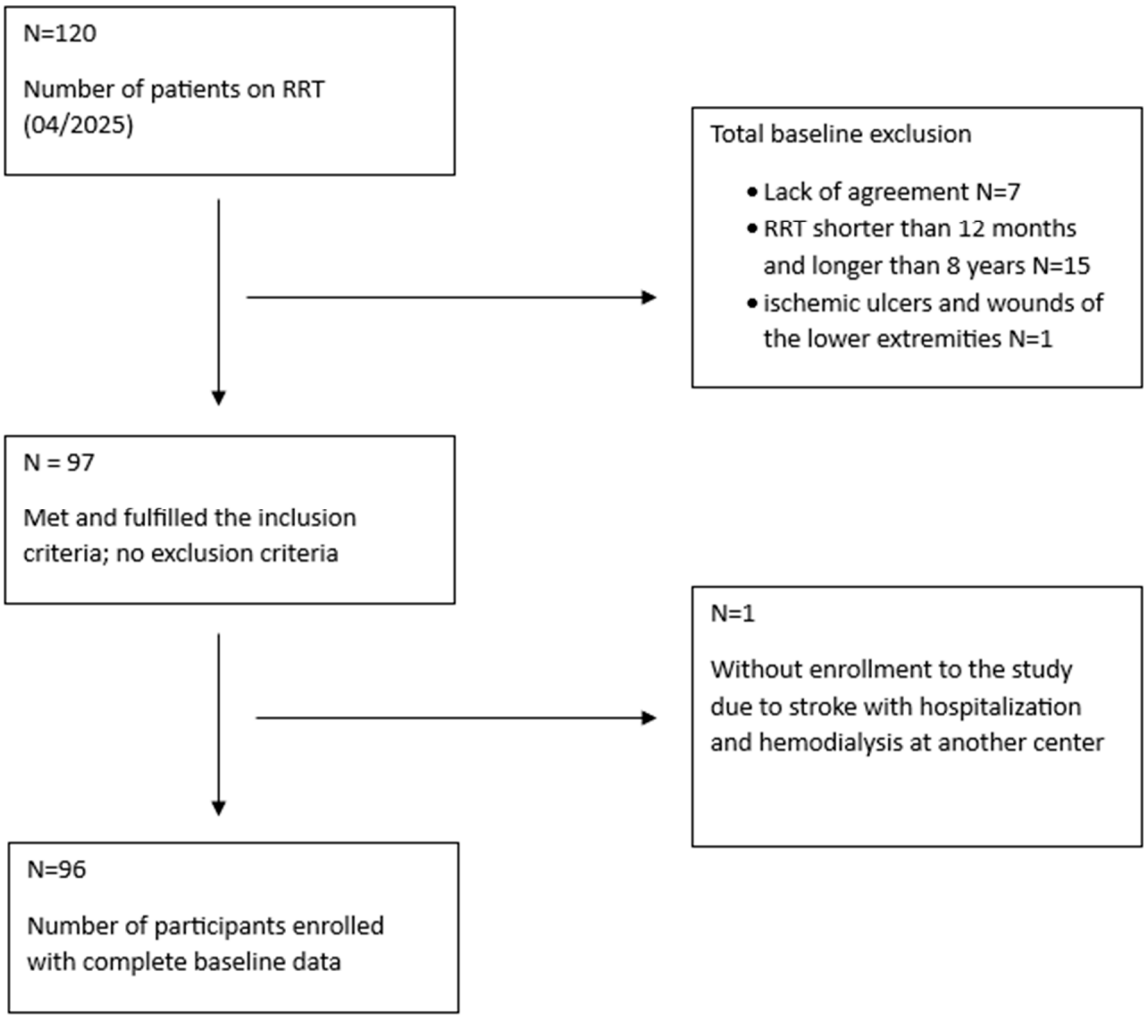

Body Composition Analysis

Body composition was assessed using a validated medical bioimpedance analyzer (seca mBCA 525, SECA GmbH, Germany), according to the manufacturer's instructions [19]. Body weight and height were measured manually prior to bioimpedance analysis. Measurements were performed after a hemodialysis session to minimize the effect of fluid overload. The examination was rapid and non-invasive, based on an 8-point bioelectrical impedance measurement. The applied current was 100 μA. Due to safety considerations, patients with implanted cardiac devices were excluded.

Parameter	Description
BMI—body mass index [kg/m²]	A value derived from body mass divided by the square of the body height, traditionally used to group individuals as underweight, normal, overweight or obese.
FFM—fat free mass [kg], relative to weight [%]	Calculated by subtracting body fat weight from total body weight; also referred to as "lean body mass".

 doi:10.20944/preprints202604.0227.v1

FFMI—fat free mass index [kg/m²]	Describes the amount of fat-free mass ("lean body mass") in relation to height and weight. Similar to BMI.
FM—fat mass [kg], relative to weight [%]	Total amount of fat; percentage of total bodyweight that is fat.
FMI—fat mass index [kg/m²]	Describes the amount of fat mass in relation to height and weight. Similar to BMI.
TBW—total body water [l], relative to weight [%]	The sum of intracellular water and extracellular water volume; approx. 60% of body weight of a normovolemic individual.
Phase angle φ [°]	Calculated by reactance/resistance ratio during bioelectrical impedance measurement. Used as an indicator of cell wall stability. Helpful in health risk assessment.
VAT—visceral adipose tissue [l]	Also known as abdominal fat, describes adipose tissue that surrounds the organs in the abdominal cavity. Overdeposition of visceral fat in the abdomen is known as visceral obesity.

Body composition assessment was performed using a rapid and non-invasive 8-point bioelectrical impedance analysis conducted on the patient's body surface. The electrical current applied during the measurement was 100 μA; therefore, individuals with implanted cardiac electronic devices were excluded for safety reasons. To minimize the influence of fluid overload, all measurements were performed immediately after a hemodialysis session.

Participants were categorized according to body mass index (BMI) into standard clinical groups: starvation (< 16.0 kg/m²), emaciation (16.0–16.99 kg/m²), underweight (17.0–18.49 kg/m²), normal weight (18.5–24.99 kg/m²), overweight (25.0–29.99 kg/m²), obesity class I (30.0–34.99 kg/m²), obesity class II (35.0–39.99 kg/m²), and obesity class III (> 40.0 kg/m²).

The SECA body composition analyzer automatically classified results according to reference ranges adjusted for age, sex, ethnicity, and BMI. Fat mass index (FMI) was categorized as low, normal, elevated, or high, while visceral adipose tissue (VAT) was classified as decreased, normal or increased. Phase angle values were interpreted as reduced (<5°), normal (5–7°), or elevated (>7°), reflecting cellular integrity and membrane function.

Fat-free mass index (FFMI) was analyzed separately for women and men using sex-specific reference values [20]. In women, values below 14 kg/m² were considered below average, 14–18 kg/m² as normal, and above 18 kg/m² as high. In men, values below 18 kg/m² were classified as below average, 18–25 kg/m² as normal, and above 25 kg/m² as high muscle mass.

Inflammatory and Nutritional Markers

Blood samples were collected prior to the hemodialysis session during routine monthly laboratory assessments. Samples were obtained from the arteriovenous fistula or dialysis catheter after withdrawal of the locking anticoagulant solution. Blood was drawn into 4 mL EDTA tubes, centrifuged at 4000 rpm for 10 minutes, and plasma was stored at −80°C until further analysis.

Inflammatory status was assessed by measuring high-sensitivity C-reactive protein (hsCRP), interleukin-6 (IL-6), interleukin-1β (IL-1β), and tumor necrosis factor-α (TNF-α).

Plasma concentrations of classical inflammatory markers were measured using commercially available enzyme-linked immunosorbent assay (ELISA) kits. Quantikine HS ELISA kits (Bio-Techne R&D Systems, Abingdon, UK) were used for the determination of hs IL-6, hs IL-1β, and hs TNF-α. Hs CRP concentrations were determined using ELISA kits from DRG Instruments GmbH (Marburg,

 doi:10.20944/preprints202604.0227.v1

Germany). All analyses were performed according to the manufacturers' protocols. Absorbance measurements were carried out using a BioTek Cytation 5 Cell Imaging Multimode Reader.

The concentrations of nutritional status markers: albumin, transferrin were obtained from routine biochemical tests performed in the Central Laboratory of the University Clinical Hospital No. 2, Pomeranian Medical University in Szczecin.

Nutritional and inflammatory burden was further assessed using the Malnutrition-Inflammation Score (MIS), as originally described by Kalantar-Zadeh et al. [21]. The MIS incorporates elements of medical history (including weight changes, appetite, gastrointestinal symptoms, and functional capacity), physical examination findings related to fat and muscle wasting, body mass index (BMI), and laboratory parameters such as albumin and transferrin levels. A total MIS score was calculated for each participant.

Eight-Month Follow-Up

All paticipants were prospectively followed for eight months. During this period, all-cause mortality, cardiovascular mortality, and the occurrence of major adverse cardiovascular events (MACE) were recorded. MACE included hospitalization due to heart failure, myocardial infarction, stroke, limb ischemia requiring hospitalization, and cardiovascular death. Patients who underwent kidney transplantation during follow-up were censored at the time of transplantation.

Clinical and Laboratory Data

Demographic and clinical data were collected for each participant, including age, sex, dialysis vintage, type of vascular access, dialysis adequacy (Kt/V), primary cause of CKD, comorbidities (including cardiovascular disease, diabetes, malignancy, chronic obstructive pulmonary disease, and autoimmune disorders), and current medication use.

Routine laboratory parameters analyzed included hemoglobin, ferritin, transferrin, albumin, calcium, phosphate, and parathyroid hormone (PTH).

No participants met KDIGO criteria for erythropoiesis-stimulating agent (ESA) resistance, defined as an erythropoietin (EPO) dose exceeding 300 IU/kg/week subcutaneously or 450 IU/kg/week intravenously without adequate hemoglobin response. Therefore, the erythropoietin resistance index (ERI) was used as a continuous measure of ESA responsiveness.

ERI was calculated as the mean weekly EPO dose per kilogram of body weight divided by the mean hemoglobin concentration (g/dL), based on values obtained over the preceding three months. As no universally accepted ERI cut-off exists to define ESA hyporesponsiveness, patients were analyzed according to median values and tertiles.

Bioinformatics

The bioinformatic methodology eployed in this study encompasses a comprehensive and reproducible analysis of full-length 16S rRNA marker sequences and it was fine tuned to the sequencing parameters

Preprocessing

Basecalling

The initial preprocessing phase was taking its place simultaneously to the sequencing on Oxfor Nanopore Technologies Promethion 2 Integrated. The sequencer itself allows for robust utilization of dual flowcell configuration. The *real-time basecalling* was performed on the HAC (High ACcuracy) *dorado* model (5.2.0, 400 bps). The choice of HAC models for *real-time basecalling* was dictated by the hardware bottleneck of the NVIDIA A100GPU (Graphics Processing Unit) onboard the Promethion 2 Integrated, which cannot handle *real-time basecalling* on a dual flowcell setup with SUP (SUPer accuracy) basecalling models, due to insufficient processing capacity that introduces lags to the sequencing summary [https://github.com/Kirk3gaard/2025-Crowdsource-GPU-basecalling-stats]. Despite the induced processing delays, the implementation of real-time basecalling was methodologically necessary. This approach provided the crucial advantage of continuous monitoring of barcode abundance and library uniformity throughout the sequening []. Such real-time evaluation was strictly required to determine the optimal operational termination point of the sequencing run,

 doi:10.20944/preprints202604.0227.v1

allowing the sequecning to be strategically stopped, when the evaluated samples successfully reached the lowest acceptable passed reads threshold (70000 reads).

Following the initial basecalling, the raw POD5 files were basecalled with use of the standardized *wf-basecalling* pipeline (version 1.5.7) from the EPI2ME framework (version 5.3.1), utilizing the SUP basecalling model (5.2.0). The pipeline was configured to trim all the adapters and barcodes from the SQK-16S114-24 barcoding kit, present in the data.

Processing

Curation of metadata

The collected metadata were stored in form of XLSX sheet and curated using the Python libraries *Pandas* (2.2.2) and *Numpy* (1.26.4). The columns regarding anthropometric indices were processed from continuous to factorial, using following constraints:

1. **Body Mass Index (BMI):** categorized into starvation (< 16.0 kg/m²), emaciation (16.0–16.99 kg/m²), underweight (17.0–18.49 kg/m²), normal weight (18.5–24.99 kg/m²), overweight (25.0–29.99 kg/m²), obesity class I (30.0–34.99 kg/m²), obesity class II (35.0–39.99 kg/m²), and obesity class III (> 40.0 kg/m²).
2. **Fat Mass Index (FMI):** divided into four levels: low, normal, elevated, and high, as specified in the database.
3. **Visceral Adipose Tissue (VAT):** classified into three categories: normal, elevated, and high.
4. **Phase Angle:** grouped into three ranges: decreased (< 5°), normal (5–7°), and increased (> 7°).
5. **Fat-Free Mass Index (FFMI):** segmented by gender with specific cutoff points.

- For **females**: below average (< 14 kg/m²), good muscle mass (14–18 kg/m²), and high muscle mass (> 18 kg/m²).
- For **males**: below average (< 18 kg/m²), average (18–25 kg/m²), and high (> 25 kg/m²).

The continuous variables presenting given metrics were also utilized in this study, at stages where continuous variables are required (e.g alpha-diversity correlation).

Analysis with standardized wf-16s pipeline from EPI2ME framework

To validate the sequencing and explore whether samples make biological sense, the wf-16s pipeline (1.6.0) was run, configured to perform taxonomical classification to the SILVA 138.1 database (EPI2ME had no default option to use SILVA 138.2 database) with use of the *minimap2* aligner [22] . The reports were thoroughly examined in search for outliers. The *wf-16s* pipeline does not take into account phylogenetic analysis and statistical testing in its alpha-diversity and beta-diversity analysis, thus the later employment of different approach was necessary.

Quality Control and Filtering

Quality control and filtering for the data coming from ONT long-read sequencing, require dedicated tools such as the *NanoPlot* (1.46.2) and *NanoFilt* (2.8.0) used to present the quality control results and to filter sequences according to specified parameters [23].

The initial quality control have been done on unlfiltered data, to check the read length and read quality distributions across all samples, investigating each sample single handedly and by creating bulk report with MultiQC (1.33) [24]. The minimal read length threshold was set to 800 base pairs, maximal read length threshold was set to 2200 base pairs, to remove clear artifacts from the generated data, but they turned out to be arbitrary as the range of length revlolved around conservative 1500 base pairs, meaning that the sequencing did not produced any artifacts. The quality threshold was set to a PHRED score of 12, as the amount of data below that threshold made about 5% of generated reads, and the mean PHRED score of raw data equaled 24.3 with 114400 reads per sample on average.

After quality filtering with NanoFilt, the second round of quality control with NanoPlot and MultiQC took place, giving sequences with a mean PHRED score of 24.3 with 113500 reads per sample on average.

Preparation for Analysis with Qiime2

As the quality of data coming from the SUP model basecalling does not require any read correction, and denoising methods such as DADA2 or Deblur are incompatible with them, the pre-processed BAM files were converted to FASTA, as sequences of high fidelity and certainty. To be able

 doi:10.20944/preprints202604.0227.v1

to fully utilize the *Qiime2* framework, the ONT sequenced data coming from the complementary strand needs to be rewritten to match the original template strand with `vsearch orient`, using SILVA 138.2 SSU Ref NR99 database. The FASTA files records headers were then signed with the corresponding sample ID, and the sample manifest in TSV format was prepared to serve as an input for the Qiime2 framework.

Downstream Analysis

The downstream analysis was performed fully using Qiime2 2026.1 (rachis) framework with Python API.

OTU Construction and Sequence Processing with Vsearch

The OTU construction and sequence clustering was performed using the `vsearch` plugin [25], using the dereplication action `dereplicate-sequences`, chimera filtering using action `uchime-ref`, and clustered to the reference database using`cluster_sequences_closed_ref` action with the identity threshold set to 97% and abundance threshold set to a minimum of 1. Only the sequences clustered to the reference were passed onto the next steps of the analysis.

The SILVA 138.2 reference database was downloaded with use of the `rescript` plugin and processed with constraints set to eliminate the eucaryotic, fungal and viral artifacts, sequences of lower quality with a number of degenerate nucleotides higher than 5, sequences with homopolymers longer than 8, and standard SILVA 138.2 taxonomy parsing [26].

Construction of Phylogenetic Tree

The phylogenetic tree, to use for phylogenetic alpha-diversity and beta-diversity metrics, was constructed with use the `phylogeny` plugin using the `align-to-tree-mafft-fasttree` pipeline on the sequences clustered to the reference at the OTU construction step [27,28].

Exploratory Data Analysis

To learn about hidden data properties, such as confounding factors, the exploratory data analysis has been performed on the whole dataset, without any stratification.

Diversity Analysis

Diversity analysis was performer using `diversity` plugin including the alpha rarefaction curves to find the minimal acceptable sampling depth for phylogenetic analysis; beta rarefaction curves to see how the rarefactioning affects the beta-diversity metrics; the core phylogenetic and non-phylogenetic alpha-diversity and beta-diversity metrics such as Faith Phylogenetic Diversity [29], Unweighted UniFrac [30], Weighted UniFrac [31], Bray-Curtis dissimilarity [32], Shannon entropy [33], Chao1 (*(PDF) Non-Parametric Estimation of the Classes in a Population*, n.d.), Simpson diversity index [34], Simpson dominance index [34], Gini index; alpha correlation tests, beta correlation test, alpha group significance test, beta group significance test, and multivariate analysis of variance with `adonis` action. The Principal Coordinate Analysis results, as well as the Bray-Curtis, Weighted UniFrac, and Unweighted UniFrac distance matrices, were plotted with use of the plugin `emperor [35,36] as well as their transformations to UMAP and t-SNE for thorough examination of patterns in the data.

The main confounding factor identified was the sex of the patient, and the `adonis` analysis was run in two configurations, one without taking sex info formula as an interaction factor and the second with sex taken into account for permutations of variables tested.

Stratification by Sex

The dataset has been stratified by sex, and the entire diversity analysis has been recalculated for both cohorts. The type of vascular access was detected as an interaction factor for the male cohort and thus, the two-way configuration of significance testing was also applied. The vascular access type class imbalance for the female cohort made the two-way configuration of significance testing impossible to apply.

Taxonomic Classification

The taxonomic classification was performed using pre-trained SILVA 138.2, human stool weighted scikit-learn classifier using sample sequences clustered to the SILVA 138.2 reference. The backwards compatibility between Qiime2 2026.1 and Qiime2 2025.7 allowed to use of the pre-trained

 doi:10.20944/preprints202604.0227.v1

classifier. Krona plots were generated with stratification by sex, with use of q2-krona community plugin utilizing original krona library [37].

3. Results

The analysis included patient data such as age, sex, duration of hemodialysis in months, type of vascular access (catheter or arteriovenous fistula), dialysis adequacy expressed as the KT/V index, cause of kidney failure, comorbidities including cardiovascular disease, malignancy, diabetes, COPD, and autoimmune diseases, as well as medications used. Standard laboratory parameters were also included in the analysis, such as complete blood count, ferritin, transferrin, albumin, calcium, phosphorus, and parathyroid hormone (PTH) levels.

In our study population, no cases of ESA resistance were identified according to the KDIGO definition, that is, an EPO dose greater than 300 U/kg/week subcutaneously or 450 U/kg/week intravenously without an adequate hemoglobin response. Therefore, we considered the erythropoietin resistance index (ERI) to be a better indicator of ESA response, as it incorporates the mean hemoglobin level as one of its components. As in other studies on EPO hyporesponsiveness, we compared patient groups on either side of the median and/or across tertiles, since no universally accepted ERI cutoff clearly defines EPO hyporesponsiveness. In this study, the erythropoietin resistance index was calculated as the mean weekly erythropoietin dose per kilogram of body weight divided by the mean hemoglobin concentration (g/dL), based on values recorded over the previous three months.

The study included 96 hemodialysis patients, of whom 62 were men (64.6%) and 34 were women (35.4%). The median age was 66 years, and the median dialysis vintage was 25.5 months, indicating a population of predominantly older patients with established end-stage kidney disease. According to BMI-based classification, most participants had normal body weight (44.8%), whereas 32.3% were overweight and 22.9% were obese; no underweight individuals were identified.

Body composition analysis showed a median fat mass index of 8.2 kg/m² and a median fat-free mass index of 19.3 kg/m². The median skeletal muscle mass was 25.1 kg, visceral adipose tissue volume was 2.3 L, phase angle was 4.5, and total body water content was 52.7%. Altogether, these findings suggest considerable heterogeneity in nutritional and body composition status within the study group.

The median erythropoietin resistance index was 9.27 IU/kg/g/dL/week. Inflammatory markers showed a median IL-6 concentration of 6.92 pg/mL, hsCRP of 4.5 mg/L, IL-1β of 0.04 pg/mL, and TNF-α of 2.77 pg/mL, indicating the presence of low-grade systemic inflammation in a substantial proportion of patients. The median albumin concentration was 40 g/L and the median transferrin concentration was 1.76 g/L. Dialysis adequacy was acceptable, with a mean Kt/V of 1.29. The median total MIS score was 5, reflecting a generally mild to moderate burden of malnutrition-inflammation risk across the cohort.

The relative abundance profiles at the genus taxonomic rank revealed marked inter-individual variability in microbial community composition. The communities were primarily composed of taxa belonging to the genera Blautia, Faecalibacterium, Streptococcus, Gemmiger, Ruminococcus, Escherichia-Shigella, and Enterococcus. While some samples were dominated by taxa commonly associated with core gut microbiota, others showed an increased contribution of potentially opportunistic genera, including Escherichia-Shigella, Streptococcus, and Enterococcus, indicating substantial compositional heterogeneity across the cohort (Figure 1).

Among the analyzed clinical and body composition variables, only sex was significantly associated with alpha diversity measured by the Chao1 index, with higher richness observed in men than in women (Figure 2, $H = 4.38$, $p = 0.036$). No significant differences were detected for phase angle, VAT class, FFMI class, FMI class, or BMI class (all $p > 0.05$), suggesting that microbial richness was relatively stable across the examined nutritional and body composition strata.

 doi:10.20944/preprints202604.0227.v1

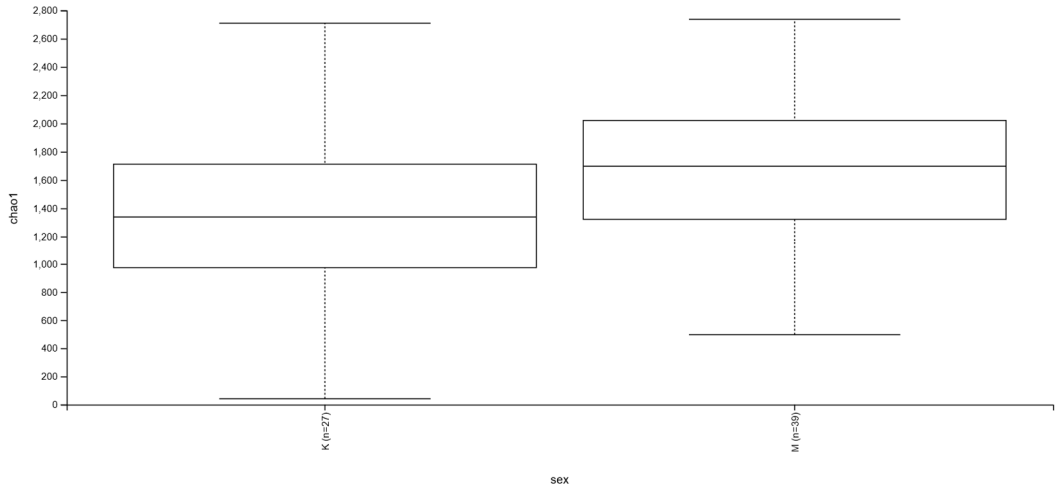

Figure 2. Alpha diversity (Chao1 index) across sex and selected body composition categories. A significant difference was observed between males and females, with higher richness in men, whereas no significant differences were found across phase angle, VAT, FFMI, FMI, or BMI categories. Statistical comparisons were performed using the Kruskal-Wallis test.

Beta-diversity analysis revealed a significant difference in overall microbial community structure between groups K and M, as demonstrated by PERMANOVA (pseudo-F = 1.4658, p = 0.014, 999 permutations; n = 54). These findings indicate that the centroids of the two groups differed significantly in multivariate space, suggesting compositional separation between K and M.

In the alpha-diversity analyses, several significant associations with age and visceral adipose tissue (VAT) were observed. Shannon entropy showed positive correlations with both age (Spearman's rho = 0.3626, p = 0.0071, n = 54) and scaled VAT values (rho = 0.3151, p = 0.0203, n = 54), indicating higher diversity in older participants and in individuals with greater visceral adiposity. Similarly, Chao1 richness was positively correlated with age (rho = 0.2946, p = 0.0172, n = 65) and scaled VAT (rho = 0.2779, p = 0.0250, n = 65). Faith's phylogenetic diversity also increased with age (rho = 0.3173, p = 0.0194, n = 54).

In contrast, the Gini index showed negative correlations with both age (rho = -0.3402, p = 0.0056, n = 65) and scaled VAT (rho = -0.2881, p = 0.0199, n = 65), suggesting reduced community inequality with increasing age and visceral adiposity. Overall, these results indicate that both age and VAT were associated with greater microbial richness and diversity, accompanied by a more even community structure.

In the female subgroup, beta-diversity analysis demonstrated significant differences in microbial community composition across the three categories ("normal", "high", and "elevated"), as shown by PERMANOVA (pseudo-F = 1.3416, p = 0.010, 999 permutations). This finding indicates that the overall gut microbiota structure differed significantly between women classified into these categories.

Inspection of the group significance plots suggested partial separation of the female subgroups in multivariate space. The "elevated" category appeared to be the most distinct, whereas the "high" and "normal" groups showed greater overlap in their distance distributions. Overall, these findings support the presence of significant, although moderate, compositional differences in the gut microbiota among women across the analyzed categories (Figure 3).

 doi:10.20944/preprints202604.0227.v1

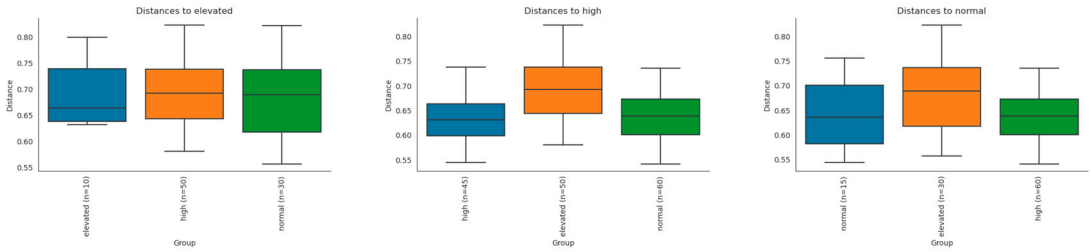

Figure 3. Beta-diversity differences among women stratified into the "normal", "high", and "elevated" categories. Overall group separation was assessed using PERMANOVA with 999 permutations. Boxplots show distances to group centroids, illustrating differences in microbial community composition between female subgroups.

The Mantel test revealed a significant positive correlation between the microbiota distance matrix and the metadata distance matrix (Spearman's rho = 0.2414, p = 0.038; 999 permutations). This finding suggests that greater differences in metadata were associated with greater dissimilarity in gut microbial composition. However, the analysis was restricted to 21 shared samples because 44 IDs were excluded from both matrices before testing (figure 4).

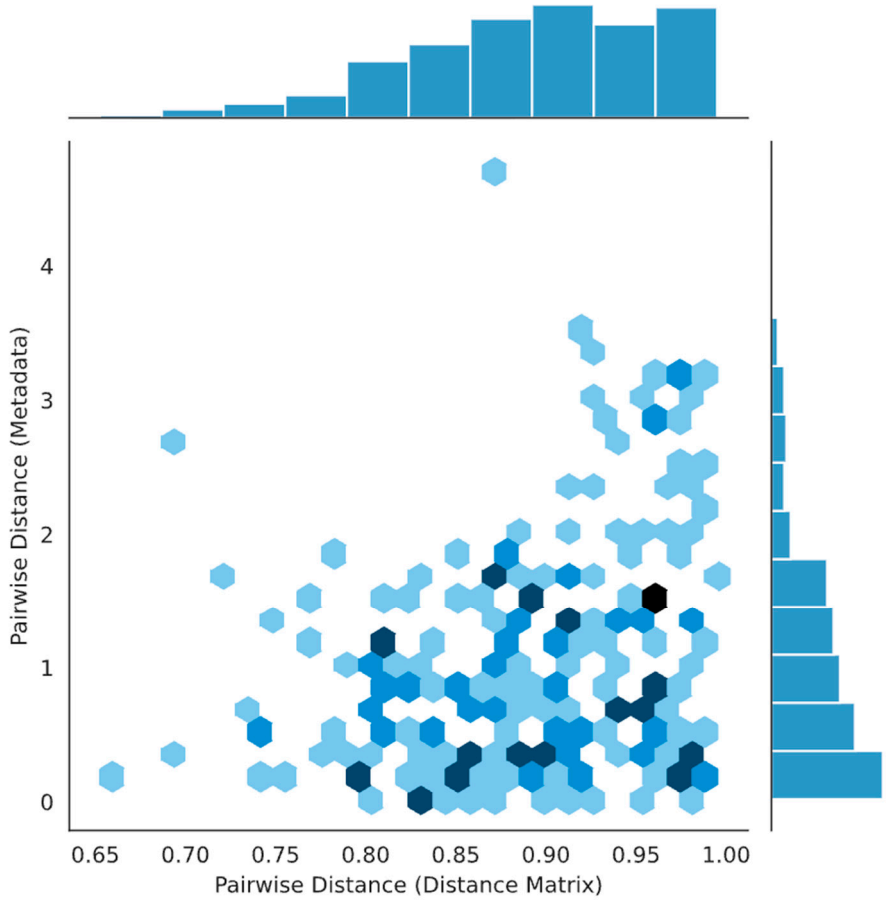

Figure 4. Mantel test assessing the association between the microbiota distance matrix and the metadata distance matrix. A positive correlation was observed between the two matrices (Spearman's rho = 0.2414, p = 0.038; 999 permutations), indicating that larger differences in metadata were associated with greater differences in microbial community composition. The analysis was performed on 21 samples shared between both matrices.

4. Discussion

 doi:10.20944/preprints202604.0227.v1

In this study, we characterized the gut microbiota of maintenance hemodialysis patients in relation to demographic, nutritional, inflammatory, and body composition parameters. Several findings deserve emphasis. First, the microbiota showed marked inter-individual heterogeneity at the genus level, with profiles ranging from communities enriched in taxa commonly regarded as part of the core gut microbiota to profiles with a greater contribution of potentially opportunistic genera. Second, sex was associated with microbial richness, with higher Chao1 values in men than in women, and overall community composition also differed between the two sex groups. Third, age and visceral adipose tissue (VAT) were positively associated with several alpha-diversity metrics, whereas the Gini index showed inverse associations, suggesting a more even microbial community structure in older individuals and in those with greater visceral adiposity. Fourth, in women, beta-diversity differed across the analyzed categories, indicating possible sex-specific host-microbiota relationships. Finally, the positive Mantel test suggested that broader clinical dissimilarity between patients was modestly reflected in microbiota dissimilarity.

These observations fit the broader concept of the gut-kidney axis, in which chronic kidney disease and kidney failure are linked to altered intestinal ecology, impaired barrier function, systemic inflammation, and the accumulation of gut-derived uremic solutes. Prior work in kidney disease has shown that CKD itself alters intestinal microbial structure, while more recent nephrology reviews have emphasized that uremia, inflammation, medication exposure, and dietary restriction all contribute to microbiome variation in CKD and dialysis populations. Accordingly, microbiome patterns in hemodialysis should probably be interpreted less as a simple healthy-versus-unhealthy dichotomy and more as a dynamic ecological response to the combined pressures of kidney failure, dialysis treatment, and host phenotype [38–41].

The marked between-patient heterogeneity observed in our cohort is also biologically plausible in light of prior dialysis-specific data. In a comparative study of patients undergoing hemodialysis or peritoneal dialysis, Stadlbauer et al. reported an increase in potentially pathogenic species and a decrease in beneficial species, with compositional changes in hemodialysis additionally associating with C-reactive protein. That framework is consistent with our finding that some samples were dominated by genera such as Blautia or Faecalibacterium, whereas others showed a greater contribution of Escherichia-Shigella, Streptococcus, or Enterococcus. Importantly, because our data are based on genus-level resolution, these taxa should not be overinterpreted functionally; rather, they support the view that the hemodialysis microbiome is compositionally unstable and clinically heterogenyeous [41,42].

The sex-associated findings are particularly interesting. Men showed higher Chao1 richness than women, and beta-diversity analyses suggested overall compositional separation between the two groups. Recent large-cohort microbiome work has shown that sex-related differences in gut microbiota are generally modest and are often strongly influenced by covariates, including age, menopause, and other host factors. Even so, these differences may still be relevant in clinical populations, especially when sex is linked to differences in body composition, fat distribution, immune tone, and treatment exposure. In the present cohort, the combination of alpha- and beta-diversity findings suggests that sex should not merely be treated as a nuisance covariate, but rather as a biologically relevant stratifier in future dialysis microbiome studies [41–43].

The positive association between age and alpha-diversity metrics requires careful interpretation. In the ageing literature, the gut microbiome is recognized as an important modulator of health across the lifespan, but age-related microbiome changes are not uniform and are influenced by diet, medications, physiology, and broader lifestyle-related factors. Moreover, recent work in healthy adults has shown that gut physiology, including transit time and luminal pH, is a major determinant of inter-individual microbiome variation. In this context, the higher Shannon, Chao1, and Faith's phylogenetic diversity observed in older patients in our cohort should not be interpreted automatically as a marker of a "healthier" microbiome. In a dialysis setting, higher diversity may just as plausibly reflect ecological restructuring under chronic disease conditions, including the coexistence of commensal and opportunistic taxa. Thus, the age-related signal identified here is

 doi:10.20944/preprints202604.0227.v1

probably best understood as a marker of altered microbiome organization rather than a direct indicator of microbiological benefit [42,44,45].

A similarly cautious interpretation is needed for the associations with visceral adipose tissue. In our study, higher VAT was associated with greater richness and diversity and with lower Gini index values, suggesting a more even distribution of taxa. At first glance, this may appear counterintuitive because obesity is often discussed in the context of microbiome disruption. However, recent large-scale human data indicate that gut microbiome composition and function are associated with multiple metabolic health measures, while experimental work has shown that obesity-associated microbiomes can be linked specifically to visceral adipose tissue inflammation. These observations suggest that adiposity-related microbiome shifts are not adequately captured by simplistic "high diversity good, low diversity bad" narratives. In hemodialysis patients, VAT may reflect not only metabolic burden but also nutritional reserve, inflammatory activity, and broader body-composition phenotype. Therefore, our VAT-related findings likely point to a host-microbiota-metabolic interaction that is real but clinically complex [46,47].

The female subgroup analysis strengthens the possibility that host-microbiota relationships differ by sex. Among women, beta-diversity differed across the analyzed categories, with the "elevated" subgroup appearing the most distinct. Given the growing recognition that sex-stratified microbiome patterns can be subtle but meaningful, this result is worth retaining in the manuscript. At the same time, it should be framed as exploratory, particularly because subgroup numbers were limited and the biological interpretation depends heavily on the exact clinical variable used to define the "normal", "high", and "elevated" categories. The main value of this analysis is therefore not that it proves a sex-specific mechanism, but that it supports sex-aware hypothesis generation for future studies [43,48].

The Mantel test adds another layer to the interpretation. Rather than linking the microbiome to a single parameter, it suggests that overall clinical distance between patients is mirrored, at least modestly, by overall microbiota distance. This idea is consistent with the broader literature showing that human gut microbiome individuality emerges from the combined effects of host physiology, environment, and metabolic phenotype rather than any single variable alone. However, this result should be interpreted conservatively in our study, because the analysis was restricted to only 21 shared IDs after exclusion of unmatched samples. Accordingly, the Mantel result is better viewed as supportive evidence of multidimensional host-microbiota coupling than as a definitive standalone finding [49,50].

Several limitations should be acknowledged. First, the cross-sectional design prevents causal inference. Second, the study was based on a single dialysis cohort without a healthy control group or a non-dialysis CKD comparator. Third, the analysis was performed at the genus level, which limits mechanistic interpretation. Fourth, some associations were detected in relatively small subgroups, and several findings should be regarded as exploratory, especially in the absence of a clearly reported multiple-testing correction strategy. Fifth, the Mantel analysis was based on a reduced set of shared samples. Finally, although ERI was an important clinical phenotyping variable in this study, the microbiome signals identified here aligned more clearly with sex, age, and body-composition parameters than with ESA responsiveness per se.

Despite these limitations, the study has several strengths. The cohort was clinically well characterized, with simultaneous assessment of inflammatory markers, nutritional indicators, dialysis adequacy, body composition, and ERI. This multidimensional phenotyping is important because current nephrology and microbiome literature increasingly argues that CKD-associated dysbiosis should be analyzed in the context of host metabolic and inflammatory state rather than as an isolated sequencing readout. In addition, the inclusion of bioimpedance-derived markers such as VAT, phase angle, FMI, and FFMI adds clinically meaningful granularity beyond BMI alone [49,51,52].

5. Conclusions

 doi:10.20944/preprints202604.0227.v1

In conclusion, our results suggest that the gut microbiota of hemodialysis patients is highly heterogeneous and associated primarily with sex, age, visceral adiposity, and broader host phenotype. These associations are statistically modest but biologically plausible and support the view that microbiome variation in dialysis reflects the combined influence of demographic, physiological, metabolic, and treatment-related factors. Future studies should validate these findings in larger, longitudinal, and sex-stratified cohorts, incorporate dietary and medication data more explicitly, and extend the analysis toward species-level and functional profiling to better define the clinical relevance of microbiota alterations in end-stage kidney disease.

6. Strengths

The study group was assessed not only with a nutritional questionnaire, but also with examination of body composition. Erythropoietin resistance was calculated over 3 months of treatment.

7. Limitations

This study involved was a single-center study. . Follow-up to assess overall mortality lasted only 8 months.

Author Contributions: For research articles with several authors, a short paragraph specifying their individual contributions must be provided. The following statements should be used: “Conceptualization, KB, EK and BG.; methodology, KB, BG, VD.; software, AO.; validation, BG, MK, KM, PO; formal analysis, LD.; investigation, KB, EK.; resources, KB, EK, ACP.; data curation, BG.; writing—original draft preparation, KB, BG, EK.; writing—review and editing, LD, EK.; visualization, BG, AO.; supervision, LD.; project administration, KB, EK.; funding acquisition, EK. All authors have read and agreed to the published version of the manuscript.”.

Funding: Publication as part of project no. KPOD.07.07-IW.07-0025/24 entitled "Epigenetic calculator of the risk of major cardiovascular events among patients with chronic kidney disease undergoing hemodialysis treatments." implemented under the National Recovery and Resilience Plan, Component D "Efficiency, accessibility and quality of the health care system," Investment D3.1.1 "Comprehensive development of research in the field of medical and health sciences."

Institutional Review Board Statement

The study was conducted according to the guidelines of the Declaration of Helsinki and obtained positive opinion of the Bioethical Committee of Pomeranian Medical University in Szczecin KB-006/17/2025.

Informed Consent Statement: Informed consent was obtained from all subjects involved in the study.

Data Availability Statement: For additional data, please contact ewa.kwiatkowska@pum.edu.pl

Conflicts of Interest: The authors declare no conflict of interest

Abbreviations

The following abbreviations are used in this manuscript:

16S rRNA - 16S ribosomal RNA
BAM - Binary Alignment/Map
BMI - body mass index
CKD - chronic kidney disease
COPD - chronic obstructive pulmonary disease
CRP - C-reactive protein
EDTA - ethylenediaminetetraacetic acid
ELISA - enzyme-linked immunosorbent assay

 doi:10.20944/preprints202604.0227.v1

EPO - erythropoietin
ERI - erythropoietin resistance index
ESA - erythropoiesis-stimulating agent
ESRD - end-stage renal disease
FASTA - Fast-All sequence format
FFM - fat-free mass
FFMI - fat-free mass index
FM - fat mass
FMI - fat mass index
HAC - high accuracy
HD - hemodialysis
HRT - hydraulic retention time
hsCRP - high-sensitivity C-reactive protein
IL-1β - interleukin-1 beta
IL-6 - interleukin-6
IQR - interquartile range
KDIGO - Kidney Disease: Improving Global Outcomes
Kt/V - dialysis adequacy index
MACE - major adverse cardiovascular events
MIA - malnutrition-inflammation-atherosclerosis
MIS - Malnutrition-Inflammation Score
ONT - Oxford Nanopore Technologies
OTU - operational taxonomic unit
PEW - protein-energy wasting
PhA - phase angle
PTH - parathyroid hormone
qPCR - quantitative polymerase chain reaction
SCFA - short-chain fatty acid
SMM - skeletal muscle mass
SUP - super accuracy
TBW - total body water
TMAO - trimethylamine N-oxide
TNF-α - tumor necrosis factor alpha
TSV - tab-separated values
UMAP - Uniform Manifold Approximation and Projection
VAT - visceral adipose tissue

References

1. Feret W, Safranow K, Ciechanowski K, Kwiatkowska Ewa. How Is Body Composition and Nutrition Status Associated with Erythropoietin Response in Hemodialyzed Patients? A Single-Center Prospective Cohort Study. J. Clin. Med.2022, 11(9), 2426;
2. Kalantar-Zadeh K, Ikizler TA, Block G, Avram MM, Kopple JD. Malnutrition–inflammation complex syndrome in dialysis patients: causes and consequences. Am J Kidney Dis. 2003;42(5):864–81.
3. Meijers B, Evenepoel P. The gut–kidney axis: indoxyl sulfate, p-cresyl sulfate and CKD progression. Nephrol Dial Transplant. 2011;26(3):759–61.
4. Vaziri ND, Wong J, Pahl M, et al. Chronic kidney disease alters intestinal microbial flora and impairs intestinal barrier. Kidney Int. 2013;83(2):308–15.
5. Ramezani A, Raj DS. The gut microbiome, kidney disease, and targeted interventions. Nat Rev Nephrol. 2014;10(7):383–97.
6. Davenport A. Improving the outcomes of vascular access infections in haemodialysis patients. Nephrol Dial Transplant. 2014;29(11):1941–6.

 doi:10.20944/preprints202604.0227.v1

7. Evenepoel P, Poesen R, Meijers B. The gut–kidney axis. Pediatr Nephrol. 2017;32(11):2005–14.
8. Vaziri ND. Emerging role of gut microbiome in chronic kidney disease: current evidence and potential therapies. Nephron. 2020;144(6):527–33.
9. Rysz J, Gluba-Brzózka A, et al. Gut microbiota, a regulator of systemic inflammation in chronic kidney disease. Int J Mol Sci. 2021;22(18):9995.
10. Kaysen GA. The microinflammatory state in uremia: causes and potential consequences. J Am Soc Nephrol. 2001;12(7):1549–57.
11. Stenvinkel P. Inflammation in end-stage renal disease: the hidden enemy. Nephrol Dial Transplant. 2006;21(11):3163–5.
12. Kalantar-Zadeh K, et al. Management of patients at risk of protein–energy wasting: ESPEN guideline on clinical nutrition in chronic kidney disease. Clin Nutr. 2019;38(1):355–72
13. Tsukamoto T., Matsubara T., Akashi Y., Kondo M., Yanagita M. Annual Iron Loss Associated with Hemodialysis. Am. J. Nephrol. 2016;43:32–38. doi: 10.1159/000444335. [DOI]
14. Harvinder G.S., Swee W.C.S., Karupaiah T., Sahathevan S., Chinna K., Ahmad G., Bavanandan S., Goh B.L. Dialysis Malnutrition and Malnutrition Inflammation Scores: Screening Tools for Prediction of Dialysis—Related Protein-Energy Wasting in Malaysia. Asia Pac. J. Clin. Nutr.
15. Wehedy E, Shatat IF, Khodor Sal. The Human Microbiome in Chronic Kidney Disease: A Double-Edged Sword. Front Med (Lausanne) 2022 Jan 17:8:790783.
16. Huang H, Chen M. Exploring the Preventive and Therapeutic Mechanisms of Probiotics in Chronic Kidney Disease through the Gut-Kidney Axis. J Agric Food Chem 2024 Apr 17;72(15):8347-8364.
17. Pantazi AC, Kassim Kassim MA, Nori W et al. Clinical Perspectives of Gut Microbiota in Patients with Chronic Kidney Disease and End-Stage Kidney Disease: Where Do We Stand? Biomedicines 2023 Sep 7;11(9):2480.
18. Laiola M, Koppe L, Larabi A. Toxic microbiome and progression of chronic kidney disease: insights from a longitudinal CKD-Microbiome Study. Gut . 2025 Sep 8;74(10):1624-1637.
19. Seca mBCA User Manual. [(accessed on 7 March 2020)]. Available online: https://www.seca.com/fileadmin/documents/manual/seca_man_525_535_en.pdf.
20. Coin A, Sergi G, Minicuci N et al. Fat-free mass and fat mass reference values by dual-energy X-ray absorptiometry (DEXA) in a 20-80 year-old Italian population Clin Nutr . 2008 Feb;27(1):87-94.
21. Kalantar-Zadeh K, Kopple JD, Humphreys MH, Block G. Comparing outcome predictability of markers of malnutrition–inflammation complex syndrome in haemodialysis patients Nephrol Dial Transplant (2004) 19: 1507–1519
22. Li, H. (2018). Minimap2: pairwise alignment for nucleotide sequences. Bioinformatics, 34(18), 3094.
23. De Coster, W., D'Hert, S., Schultz, D. T., Cruts, M., & Van Broeckhoven, C. (2018). NanoPack: visualizing and processing long-read sequencing data. Bioinformatics, 34(15), 2666–2669.
24. Ewels, P., Magnusson, M., Lundin, S., & Käller, M. (2016). MultiQC: summarize analysis results for multiple tools and samples in a single report. Bioinformatics, 32(19), 3047–3048.
25. Rognes, T., Flouri, T., Nichols, B., Quince, C., & Mahé, F. (2016). VSEARCH: A versatile open source tool for metagenomics. PeerJ, 2016(10), e2584.
26. Robeson, M. S., O'Rourke, D. R., Kaehler, B. D., Ziemski, M., Dillon, M. R., Foster, J. T., & Bokulich, N. A. (2021). RESCRIPt: Reproducible sequence taxonomy reference database management. PLOS Computational Biology, 17(11), e1009581.
27. Katoh, K., & Standley, D. M. (2013). MAFFT multiple sequence alignment software version 7: improvements in performance and usability. Molecular Biology and Evolution, 30(4), 772–780.
28. Price, M. N., Dehal, P. S., & Arkin, A. P. (2009). FastTree: computing large minimum evolution trees with profiles instead of a distance matrix. Molecular Biology and Evolution, 26(7), 1641–1650.
29. Faith, D. P. (1992). Conservation evaluation and phylogenetic diversity. Biological Conservation, 61(1), 1–10.
30. Lozupone, C., & Knight, R. (2005). UniFrac: A new phylogenetic method for comparing microbial communities. Applied and Environmental Microbiology, 71(12), 8228–8235.

 doi:10.20944/preprints202604.0227.v1

31. Lozupone, C. A., Hamady, M., Kelley, S. T., & Knight, R. (2007). Quantitative and qualitative β diversity measures lead to dif-ferent insights into factors that structure microbial communities. Applied and Environmental Microbiology, 73(5), 1576–1585.
32. Bray, J. R., & Curtis, J. T. (1957). An Ordination of the Upland Forest Communities of Southern Wisconsin. Ecological Monographs, 27(4), 325–349.
33. Shannon, C. E. (1948). A Mathematical Theory of Communication. Bell System Technical Journal, 27(3), 379–423.
34. Simpson, E. H. (1949). Measurement of Diversity. Nature 1949 163:4148, 163(4148), 688–688.
35. Vázquez-Baeza, Y., Pirrung, M., Gonzalez, A., & Knight, R. (2013). EMPeror: A tool for visualizing high-throughput microbial community data. GigaScience, 2(1).
36. Vázquez-Baeza, Y., Gonzalez, A., Smarr, L., McDonald, D., Morton, J. T., Navas-Molina, J. A., & Knight, R. (2017). Bringing the Dynamic Microbiome to Life with Animations. Cell Host & Microbe, 21(1), 7–10.
37. Ondov, B. D., Bergman, N. H., & Phillippy, A. M. (2011). Interactive metagenomic visualization in a Web browser. BMC Bioin-formatics, 12(1), 385.
38. Krukowski, H., Valkenburg, S., Madella, A. M., Garssen, J., van Bergenhenegouwen, J., Overbeek, S. A., Huys, G. R. B., Raes, J., & Glorieux, G. (2023a). Gut microbiome studies in CKD: opportunities, pitfalls and therapeutic potential. Nature Reviews. Nephrology, 19(2), 87–101.
39. Lim, X., Ooi, L., Ding, U., Wu, H. H. L., & Chinnadurai, R. (2024). Gut Microbiota in Patients Receiving Dialysis: A Review. Pathogens (Basel, Switzerland), 13(9).
40. Vaziri, N. D., Wong, J., Pahl, M., Piceno, Y. M., Yuan, J., Desantis, T. Z., Ni, Z., Nguyen, T. H., & Andersen, G. L. (2013). Chronic kidney disease alters intestinal microbial flora. Kidney International, 83(2), 308–315.
41. Yang, T., Richards, E. M., Pepine, C. J., & Raizada, M. K. (2018). The gut microbiota and the brain-gut-kidney axis in hyperten-sion and chronic kidney disease. Nature Reviews. Nephrology, 14(7), 442–456.
42. Stadlbauer, V., Horvath, A., Ribitsch, W., Schmerböck, B., Schilcher, G., Lemesch, S., Stiegler, P., Rosenkranz, A. R., Fickert, P., & Leber, B. (2017). Structural and functional differences in gut microbiome composition in patients undergoing haemo-dialysis or peritoneal dialysis. Scientific Reports 2017 7:1, 7(1), 15601.
43. Vriend, E. M. C., Galenkamp, H., Herrema, H., Nieuwdorp, M., van den Born, B. J. H., & Verhaar, B. J. H. (2024). Machine learning analysis of sex and menopausal differences in the gut microbiome in the HELIUS study. Npj Biofilms and Microbiomes 2024 10:1, 10(1), 152.
44. Ghosh, T. S., Shanahan, F., & O'Toole, P. W. (2022). The gut microbiome as a modulator of healthy ageing. Nature Reviews Gastroenterology & Hepatology 2022 19:9, 19(9), 565–584.
45. Procházková, N., Laursen, M. F., La Barbera, G., Tsekitsidi, E., Jørgensen, M. S., Rasmussen, M. A., Raes, J., Licht, T. R., Dragsted, L. O., & Roager, H. M. (2024a). Gut physiology and environment explain variations in human gut microbiome composition and metabolism. Nature Microbiology 2024 9:12, 9(12), 3210–3225.
46. Keshet, A., & Segal, E. (2024a). Identification of gut microbiome features associated with host metabolic health in a large pop-ulation-based cohort. Nature Communications 2024 15:1, 15(1), 9358.
47. Shantaram, D., Hoyd, R., Blaszczak, A. M., Antwi, L., Jalilvand, A., Wright, V. P., Liu, J., Smith, A. J., Bradley, D., Lafuse, W., Liu, Y. Z., Williams, N. F., Snyder, O., Wheeler, C., Needleman, B., Brethauer, S., Noria, S., Renton, D., Perry, K. A., … Hsueh, W. A. (2024). Obesity-associated microbiomes instigate visceral adipose tissue inflammation by recruitment of distinct neu-trophils. Nature Communications 2024 15:1, 15(1), 5434.
48. Keshet, A., & Segal, E. (2024b). Identification of gut microbiome features associated with host metabolic health in a large pop-ulation-based cohort. Nature Communications 2024 15:1, 15(1), 9358.
49. Keshet, A., & Segal, E. (2024c). Identification of gut microbiome features associated with host metabolic health in a large pop-ulation-based cohort. Nature Communications 2024 15:1, 15(1), 9358.
50. Procházková, N., Laursen, M. F., La Barbera, G., Tsekitsidi, E., Jørgensen, M. S., Rasmussen, M. A., Raes, J., Licht, T. R., Dragsted, L. O., & Roager, H. M. (2024b). Gut physiology and environment explain variations in human gut microbiome composition and metabolism. Nature Microbiology 2024 9:12, 9(12), 3210–3225.
51. Evenepoel, P., Stenvinkel, P., Shanahan, C., & Pacifici, R. (2023). Inflammation and gut dysbiosis as drivers of CKD-MBD. Nature Reviews. Nephrology, 19(10), 646–657.

 doi:10.20944/preprints202604.0227.v1

52. Krukowski, H., Valkenburg, S., Madella, A. M., Garssen, J., van Bergenhenegouwen, J., Overbeek, S. A., Huys, G. R. B., Raes, J., & Glorieux, G. (2023b). Gut microbiome studies in CKD: opportunities, pitfalls and therapeutic potential. Nature Reviews. Nephrology, 19(2), 87–101.